



1N - 15 - CR

027243

**AIAA-96-3397****Near-Optimal Operation of Dual-Fuel  
Launch Vehicles****M. Ardema and H.-C. Chou****Santa Clara University****Santa Clara, CA****J. Bowles****NASA Ames Research Center****Moffett Field, CA****AIAA Atmospheric Flight Mechanics  
Conference****July 29-31, 1996 / San Diego, CA**

## Near-Optimal Operation of Dual-Fuel Launch Vehicles

M. D. Ardema\* and H.-C. Chou†  
 Santa Clara University  
 Santa Clara, California 95053

and

J. V. Bowles\*  
 NASA Ames Research Center  
 Moffett Field, California 94035

Abstract

A near-optimal guidance law for the ascent trajectory from earth surface to earth orbit of a fully reusable single-stage-to-orbit pure rocket launch vehicle is derived. Of interest are both the optimal operation of the propulsion system and the optimal flight path. A methodology is developed to investigate the optimal throttle switching of dual-fuel engines. The method is based on selecting propulsion system modes and parameters that maximize a certain performance function. This function is derived from consideration of the energy-state model of the aircraft equations of motion. Because the density of liquid hydrogen is relatively low, the sensitivity of perturbations in volume need to be taken into consideration as well as weight sensitivity. The cost functional is a weighted sum of fuel mass and volume; the weighting factor is chosen to minimize vehicle empty weight for a given payload mass and volume in orbit.

Nomenclature

$D$	= drag, lb	$LH_2$	= liquid hydrogen
$E$	= total mechanical energy per unit weight, ft	$LOX$	= liquid oxygen
$g$	= gravitational acceleration on the earth surface, ft/sec <sup>2</sup>	$M$	= Mach number
$h$	= altitude, ft	$M_{\sigma}$	= transition Mach number
$I_{sp}$	= specific impulse, sec	$M_{\sigma}^*$	= optimal transition Mach number
$K$	= weighting parameter, lb/ft <sup>3</sup>	$R$	= radius of the earth, ft
$K'$	= value of $K$ for minimum empty weight, lb/ft <sup>3</sup>	$T$	= thrust, lb
$L$	= lift, lb	$T_V$	= magnitude of thrust component along velocity vector, lb
		$t$	= time, sec
		$V$	= speed, fps
		$v_P$	= propellant volume, ft <sup>3</sup>

\* Professor and Chairman, Department of Mechanical Engineering. Associate Fellow AIAA.

† Graduate Research Assistant, Department of Mechanical Engineering. Student Member AIAA.

\* Aerospace Engineer, System Analysis Branch. Member AIAA.

$W$	= aircraft earth surface weight (mass), lb
$W_P$	= propellant earth surface weight, lb
$\phi$	= cost functional
$\eta_{HR}$	= mass flow ratio of liquid hydrogen to liquid hydrocarbon
$\eta_{OH}$	= mass flow ratio of liquid oxygen to liquid hydrogen
$\eta_{OR}$	= mass flow ratio of liquid oxygen to liquid hydrocarbon
$\rho$	= net propellant density, lb/ft <sup>3</sup>

### Subscripts

$DF$	= dual-fuel mode
$E$	= empty
$f$	= final value
$H$	= liquid hydrogen
$LO$	= lift-off
$O$	= liquid oxygen
$R$	= liquid hydrocarbon
$SF$	= single-fuel mode
$0$	= initial value

## Introduction

Current studies of single-stage-to-orbit (SSTO) launch vehicles are focused on all-rocket propulsion systems<sup>1,2</sup> (Fig. 1). One feature of a SSTO vehicle is its low payload-to-gross weight fraction. This means that vehicle performance is extremely sensitive to perturbations in vehicle design and operation. In particular, it is essential to "optimize" the flight path and the operation of the propulsion system to the extent possible in order to attain adequate mission performance, and to do this for every competing design under consideration.



Figure 1. Illustration of the SSTO rocket servicing the Hubble Space Telescope.

Dual-fuel (tripropellant) systems that initially burn both kerosene and hydrogen as fuel and later switch to solely LH<sub>2</sub>, might enable attainment of high mass fractions, principally because of their greater average propellant density and the greater thrust-to-weight ratio of LOX-kerosene engines.<sup>3-6</sup> The advantages of hydrocarbon fuel are important early in the ascent trajectory, where vehicle weight is high, and its use may be expected to lead to reduced vehicle size and weight. Because LH<sub>2</sub> is also typically needed for cooling purposes, in the early portion of the trajectory both fuels usually must be burned simultaneously. Later in the ascent, when vehicle weight is lower, specific impulse is the key parameter, indicating single-fuel LH<sub>2</sub> use.

Two recent papers<sup>5,6</sup> have considered the optimization of dual-fuel SSTO vehicles. Included in the studies was a determination of  $M_{\sigma^*}$ , the Mach Number at which to transition from dual-fuel mode to LH<sub>2</sub> operation in order to minimize vehicle empty

weight. Both of these references treat  $M_{tr}$  as an external design variable.

In this paper, a guidance algorithm is developed that determines whether dual-fuel or single-fuel operation is superior as an integral part of the trajectory integration. This approach saves a substantial number of iterations of a computer design code by reducing the number of design variables, and hence the number of design iterations required in a vehicle optimization study. Further, the guidance law will be directly useable as part of a real-time, on-board, propulsion control system.

The basis of the guidance law is the energy-state dynamic model. The key idea is to introduce the total mechanical energy as a state variable, and then to neglect all other dynamics. When flight path optimization is done with this model, simple rules for the optimal path and for the optimal operation of the propulsion system are obtained. This dynamic model has been used successfully many times to obtain effective guidance laws for a wide variety of aircraft and missions (see Ref. 7 and the references therein for a review of this work). The energy-state approach is particularly suitable for launch vehicles because efficient energy accumulation (or equivalently maximizing "total  $\Delta V$ ") is the primary trajectory optimization goal.

In a series of papers<sup>7-9</sup> we have used energy-state methods to develop algorithms for ascent trajectory optimization and optimal operation of single-fuel multi-mode propulsion systems. In particular, the operation of propulsion systems with two separate engines, air-breathing and rocket, was investigated<sup>9</sup>. The present paper extends those methods to the dual-fuel case. The main goal is to determine  $M_{tr}^*$  and to investigate optimal trajectories.

In the numerical results, vehicle performance is computed using the NASA Ames hypersonic vehicle synthesis code (HAVOC)<sup>10</sup>. HAVOC integrates geometry, aerodynamics, propulsion, structures, weights, and other computations to produce point designs for a wide variety of launch vehicles. It is capable of iteratively determining "closed" vehicles, that is, designs which meet specified payload mass and volume requirements for a specified mission. Although the trajectory guidance law is based on the energy-state model, the trajectory integration in HAVOC uses a point mass model, including the effects of earth rotation, earth curvature, and variable gravity.

### Optimization Function

The energy-state model is obtained by using the total mechanical energy per unit weight as the state variable<sup>7-9</sup>:

$$\dot{E} = P \quad (1)$$

$$\dot{W} = -\frac{T}{I_{sp}} \quad (2)$$

where

$$E = \frac{hR}{R+h} + \frac{1}{2g} V^2 \quad (3)$$

and

$$P = \frac{V}{W} (T_v - D) \quad (4)$$

and where the drag is evaluated at the lift required for equilibrium of forces perpendicular to the flight path.

For a SSTO mission, what is desired is a trajectory that gives the minimum empty weight vehicle to put a given payload mass and volume in orbit. Because the density of liquid hydrogen is low, the sensitivity of perturbations in volume need to be taken into consideration as well as mass sensitivity, and it is therefore necessary to minimize a weighted sum of propellant weight and volume. Thus we introduce the cost functional

$$\phi = W_p + K v_p \quad (5)$$

where  $K \in [0, \infty)$  is a weighting parameter to be chosen later.

The quantity to be minimized for a given energy gain is

$$J = \int_{\phi_0}^{\phi_f} d\phi = \int_{\phi_0}^{\phi_f} \dot{\phi} dt = \int_{E_0}^{E_f} \frac{\dot{\phi}}{P} dE \quad (6)$$

where Eq. (1) was used. It is assumed that  $\dot{\phi} > 0$ ,  $P > 0$  and that  $E$  is monotonically increasing. If the propellant density is  $\rho = W_p / v_p$ , then from Eqs. (2) and (5), and using  $\dot{W}_p = -\dot{W}$ ,

$$\dot{\phi} = \dot{W}_p + K \frac{\dot{W}_p}{\rho} = \frac{T}{I_{sp}} \left( 1 + \frac{K}{\rho} \right) \quad (7)$$

For convenience, we choose to invert the integrand in Eq. (6) and maximize; from Eqs. (1), (6), and (7), the quantity to be maximized is

$$J = \int_{E_0}^{E_f} F dE \quad (8)$$

where

$$F = \frac{V I_{sp} (T_v - D)}{W T \left( 1 + \frac{K}{\rho} \right)} \quad (9)$$

The guidance algorithm then consists of selecting propulsion system and trajectory parameters that maximize the function  $F$  as given by Eq. (9) at each energy level along the trajectory, subject to any relevant constraints.

For vehicles capable of either dual- or single-fuel operation, the densities to be used in Eq. (9) are

$$\rho_{DF} = \frac{\rho_R \rho_O \rho_H (1 + \eta_{OR} + \eta_{HR})}{(\rho_O \rho_H + \eta_{OR} \rho_R \rho_H + \eta_{HR} \rho_R \rho_O)} \quad (10)$$

$$\rho_{SF} = \frac{\rho_O \rho_H (1 + \eta_{OH})}{(\rho_O + \eta_{OH} \rho_H)} \quad (11)$$

SSTO vehicles are typically subject to dynamic pressure constraints and a maximum tangential acceleration limit. This latter limit, nominally 3 times the earth surface gravitational acceleration, is met by engine throttling. It may happen that the limit affects dual-fuel operation but not single-fuel operation at a point along the trajectory. All these constraints are accounted for in the guidance algorithm.

In addition to being a useful tool in preliminary design studies, the guidance algorithm should be ideal for use in an on-board real-time control system because: (1) it is fully nonlinear and models all of the vehicle's significant nonlinearities, (2) it is algebraic and thus does not rely on potentially unstable numerical integrations, and (3) it depends directly on easily measured vehicle states and parameters.

## Numerical Results

All numerical examples will be based on an SSTO rocket with a delta winged-body configuration<sup>2</sup> (Fig. 1). The three propellants (hydrocarbon fuel,  $\text{LH}_2$ , and liquid oxygen) are stored in three separate internal tanks. The vehicle takes off vertically and lands horizontally. The first results to be presented use a fixed trajectory commonly used for SSTO rockets.

As a first step, the best transition Mach number,  $M_{tr}^*$ , is determined by treating this parameter as a single external design variable, as was done in Refs. 5 and 6. The results are shown in Fig. 2, which plots gross lift-off weight ( $W_{LO}$ ) and empty weight ( $W_E$ ) as a function of  $M_{tr}$ . It is seen that both minimum  $W_{LO}$  and  $W_E$  are obtained at about  $M_{tr}^* = 9.0$ , and that the weight savings at  $M_{tr}^*$  are substantial relative to low values of  $M_{tr}$ . All of the data points on Fig. 2 are for closed vehicles and hence several design iterations are necessary for each point.

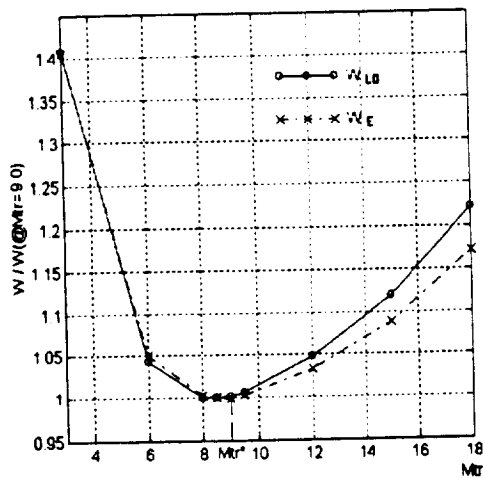


Figure 2. Effect of transition Mach number on vehicle gross take-off weight and empty weight.

Before applying the developed guidance law to this problem, the best value of  $K$  must be determined. This is done by computing

closed vehicles for a range of values of  $K$  (Fig. 3). It is evident that a value of  $K = 4$   $\text{lb/ft}^3$ , denoted hereafter by  $K^*$ , gives very nearly a minimum of both empty weight and gross lift-off weight, and this value will be used throughout the rest of the paper. This value of  $K^*$  represents a factor of over 10 in weighting the cost functional in favor of propellant mass (a value of  $K = \rho$  would signify equal weighting of propellant mass and volume.) The figure shows that the use of the optimally weighted cost functional saves 1.7% in empty weight and 1% in gross lift-off weight, relative to minimizing propellant weight only.

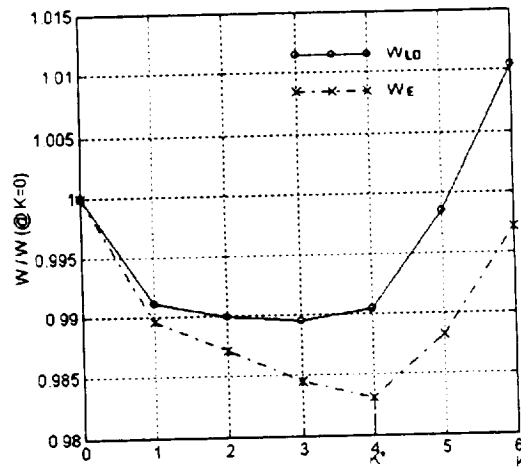


Figure 3. Variation of gross take-off weight and empty weight with parameter  $K$ .

It is of interest to compare these results with the equivalent results for an air-breathing launch vehicle, as shown in Fig. 2 of Ref. 9. For the airbreather, the best value of  $K$  is also around 4, but the empty weight reduction relative to minimizing propellant weight only is much larger, at 4.9%; this is of course because all of the airbreather propellant is low-density  $\text{LH}_2$ , and therefore this vehicle is more sensitive to volume perturbations.

Figure 4 plots the function  $F$  along the fixed trajectory. Whichever mode of operation, dual-fuel or single-fuel, that gives

the highest value of  $F$  at a given speed should be the one selected at that speed. The figure shows that from lift-off to  $M=9.0$ , the dual-fuel mode is superior, and above this speed the single-fuel mode is best. This value of  $M_{tr}^* = 9.0$  agrees with the value determined by treating  $M_{tr}$  as a design variable, Fig. 2, thus validating the guidance law. The value of  $M_{tr}^*$  as determined in Ref. 5 was in the range 8.6 - 8.9, and for Ref. 6 it was in the range 7.3 - 7.4.

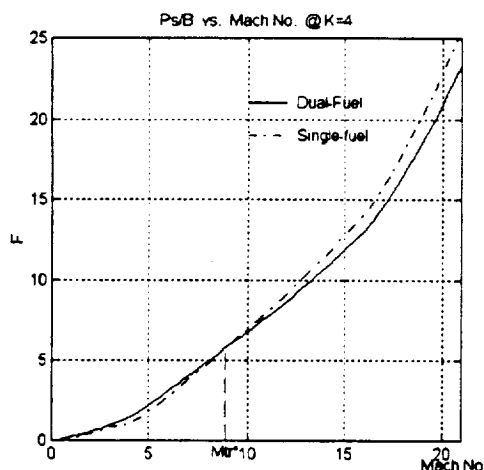


Figure 4. Cost function histories for both propulsion modes.

The relative distance between the two curves on Fig. 4 provides an assessment of the difference in performance between the two modes at a given Mach number. It is seen that both modes give substantially the same performance between  $M=7$  and  $M=11$ . This relative insensitivity to  $M_{tr}$ , characteristic of a design variable near its optimal value, was also observed in Ref. 5. The use of single fuel  $LH_2$  mode becomes increasingly advantageous as Mach number increases past 11.

Fig. 5 shows the effect of  $K$  on  $M_{tr}$ . As expected, the higher the value of  $K$ , the higher the premium on minimizing fuel volume, and thus the larger the transition Mach number,  $M_{tr}$ .

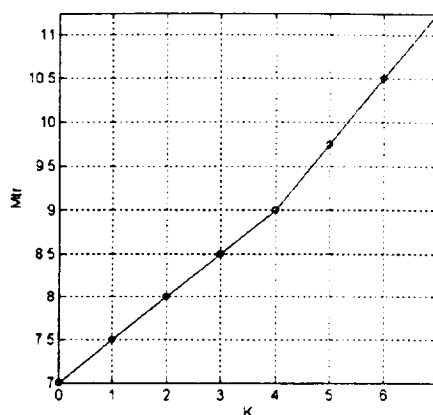


Figure 5. Effect on K on  $M_{tr}$ .

The function  $F$  was also used to optimize the ascent trajectory (Fig. 6). As compared with the fixed trajectory, the near-optimal one has increased dynamic pressure, especially in the initial dual-fuel mode.

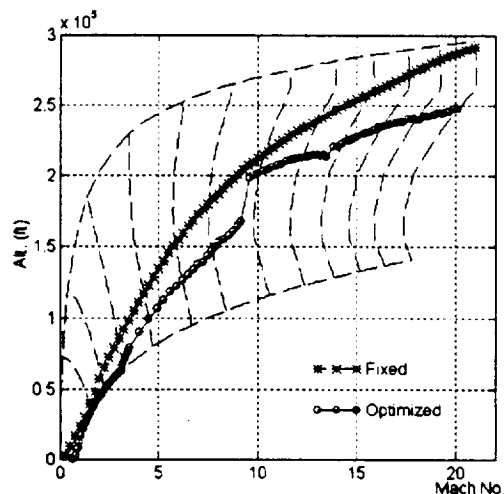


Figure 6. The fixed and optimized flight path.

Fig. 7 shows the cost function surface within the flight envelope. The optimal energy climb path begins at zero altitude and then encounters the maximum dynamic pressure boundary and begins to climb along this boundary up to Mach 3.2. After this point the trajectory increases in altitude and is not constrained by either the upper or lower dynamic pressure limits. At Mach 9.6, the tripropellant system switches to single-

fuel mode, and the altitude transits to a higher level.

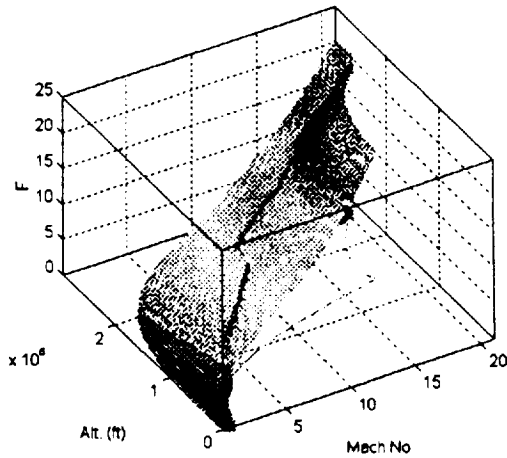


Figure 7. Cost function surface and optimized flight path.

The transition Mach number along the optimal path is equal to 9.6, as can be seen from Fig. 8.

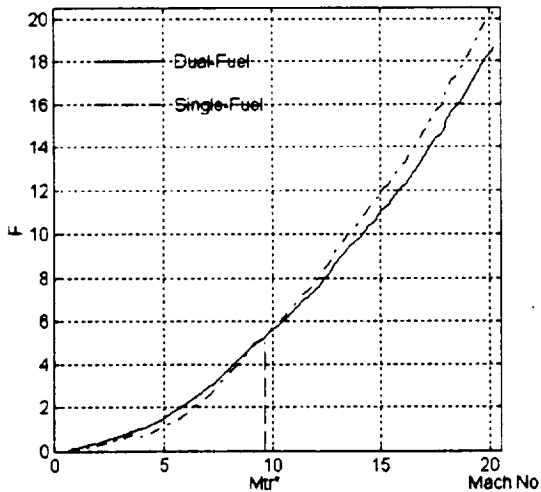


Figure 8. Cost function histories of optimal energy climb path.

Fig. 9 shows the weight ratios at each energy level. It is seen that at orbit energy level the optimal flight path gives a small but significant savings of fuel relative to the fixed path. The near-optimal trajectory consumed less fuel in the amount of 0.9% of  $W_{LO}$  than

did the fixed, almost all the difference occurring in dual-fuel mode.

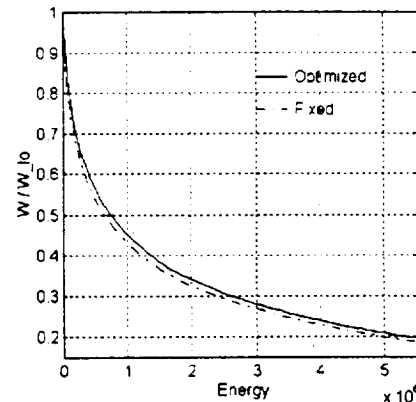


Figure 9. Weight ratios at energy levels.

### Concluding Remarks

A simple guidance law for operation of dual-fuel SSTO launch vehicles has been developed and used to determine the optimal value of the transition Mach Number from dual-fuel to single-fuel. For the example considered, the optimal transition Mach Number was 9.0 along a fixed trajectory. Along an optimal trajectory, the best transition Mach number was 9.6; the optimal trajectory had higher dynamic pressure than the fixed, particularly in dual-fuel mode.

In the future, the guidance method described in this paper easily could be extended to optimize other propulsion system parameters, such as flow rates of individual propellants in multi-propellant engines. Because the guidance algorithm is internal to the trajectory optimization routine, its use will save many iterations of a preliminary design computer code relative to treating these parameters as external design variables. The guidance law is highly accurate, robust, and simple to implement, also making it ideal for use in a real-time on-board control system for a SSTO launch vehicles.



### Acknowledgment

This work was supported by NASA Ames Research Center Grant NCC 2-5165.

### References

<sup>1</sup>Bekey, I., "SSTO Rockets; A practical Possibility," *Aerospace America*, July 1994, pp. 32-37.

<sup>2</sup>Freeman, D. C., Talay, T. A., Stanley, D. O., Lepsch, R. A., and Wilhite, A. W., "Design Options for Advanced Manned Launch Systems," *Journal of Spacecraft and Rockets*, Vol. 32, No. 2, March-April 1995, pp. 241-249.

<sup>3</sup>Salkeld, R., "Mixed-Mode Propulsion for the Space Shuttle," *Astronautics and Aeronautics*, Vol. 9, No. 8, 1971, pp. 52-58.

<sup>4</sup>Wilhite, A. W., "Optimization of Rocket Propulsion Systems for Advanced Earth-to-Orbit Shuttles," *Journal of Spacecraft and Rockets*, Vol. 17, No. 2, 1980, pp. 99-104.

<sup>5</sup>Lepsch, R. A., Stanley, D. O., and Unal, R., "Dual-Fuel Propulsion in Single-State Advanced Manned Launch System Vehicle," *Journal of Spacecraft and Rockets*, Vol. 32, No. 3, May-June 1995, pp. 417-425.

<sup>6</sup>Braun, R. D., Powel, R. W., Lepsch, R. A., Stanley, D. O., and Kroo, I. M., "Comparison of Two Multidisciplinary Optimization Strategies for Launch-Vehicle Design," *Journal of Spacecraft and Rockets*, Vol. 32, No. 3, May-June 1995, pp. 404-410.

<sup>7</sup>Ardema, M. D., Bowles, J. V., and Whittaker, T., "Optimal Trajectories for

Hypersonic Launch Vehicles," *Dynamics and Control*, Vol. 4, No. 4, 1994, pp. 337-347.

<sup>8</sup>Ardema, M. D., Bowles, J. V., Terjesen, E. J., and Whittaker, T., "Approximate Altitude Transitions for High-Speed Aircraft," *Journal of Guidance, Control, and Dynamics*, Vol. 18, No. 3, May-June 1995, pp. 561-566.

<sup>9</sup>Ardema, M. D., Bowles, J. V., and Whittaker, T., "Near-Optimal Propulsion System Operation for Air-Breathing Launch Vehicles," *AIAA Paper 94-3635, presented at the 1994 AIAA Guidance, Navigation, and Control Conf.*, Scottsdale, AZ, Aug. 1-3, 1994.

<sup>10</sup>Bowles, J. V., "Ames Conceptual Studies Activities," *Proceedings of the Second National Aerospace Plane Symposium*, Applied Physics Lab., Laurel, MD, Nov. 1986.

## Appendix B

### Approximate Methods of Trajectory Optimization

by

Mark D. Ardema



# Approximate Methods of Trajectory Optimization

Mark D. Ardema

## Introduction

Application of optimal control theory in the form of the maximum principle to aircraft trajectory optimization problems generally results in a two-point (2PBVP). The order of this problem is double the number of state variables and the equations are always “half unstable.” Many schemes have been developed to numerically solve this difficult class of problem, but all are unsuitable in a vehicle synthesis code. Not only are they computationally expensive, but they are non-robust and not user-friendly.

What is needed in a vehicle synthesis code is a method that optimizes the trajectory in one pass, that is as an integral part of the trajectory integration. The method must also be robust and it should be easy to use and to interpret physically. The key to achieving this is to use judicious approximations to reduce the functional optimization problem to a function one.

In this report, two approximation techniques are reviewed and developed. The first is the use of the Energy State Approximation (ESA). This well-known technique substitutes the total mechanical energy for the speed as a state variable, and then neglects the altitude and flight path dynamics relative to the energy dynamics. The second technique is the use of Singular Perturbation Theory (SPT) to time-scale decouple equations of motion. These two techniques are related, and in fact, the ESA may be viewed as an example of SPT methods.

## Trajectory Optimization: the Maximum Principle

The equations of motion of aircraft flight, no matter what the assumptions (see Appendix A), are of state equation form:

$$\dot{\underline{X}} = \underline{f}(\underline{X}, \underline{U})$$

where  $\underline{X} \in \mathcal{R}^n$  is the state and  $\underline{U} \in \bigcup C \mathcal{R}^m$  is the control vector. Suitable boundary conditions on the state vector components are prescribed. It is desired to find the components of  $\underline{U}$  along the trajectory so that

$$J = \int_0^{t_f} f_0(\underline{X}, \underline{U}) dt$$

is minimized. It is assumed that time is free. The necessary conditions for optimal control are provided by the Maximum Principle (MP).

Theorem (the Maximum Principle): Introduce the variational Hamiltonian function

$$H = -f_0 + \sum_{i=1}^n \lambda_i f_i$$

where the components of the adjoint vector,  $\lambda_i$ , satisfy the differential equations

$$\dot{\lambda}_i = -\frac{\partial H}{\partial X_i}; \quad i = 1, \dots, n$$

Then, if  $\underline{U}$  is an optimal control,

$$(a) \quad \underline{U} = \arg \max_{\underline{U} \in \bigcup} H$$

$$(b) \quad H = 0$$

(c) Transversality conditions (“natural” boundary conditions on the  $\lambda_i$ ) hold.

Thus, we must solve a  $2n$  dimension 2PBVP in the states and adjoints; exactly  $n$

boundary conditions are provided at  $t = 0$  and the other half at  $t = t_f$  (due to the transversality conditions). The equations are unstable in the sense that if they are linearized about a nominal trajectory, one-half of the eigenvalues will have positive real parts and the other half negative (unless they are zero).

### Approximation Techniques

Methods of reducing the 2PBVP to a simpler problem will now be developed. These methods focus on order reduction and are motivated by two simple observations.

First, we note that if all components of  $\underline{f}$ , except possibly  $f_i$ , and the function  $f_0$  are independent of a specific state variable, say  $X_i$ , and the final value of  $X_i$  is not specified, then the corresponding adjoint is always identically zero and the state equation  $\dot{X}_i = f_i$  drops out of the problem (decouples from the other states). To see this, consider the  $i^{th}$  adjoint equation and its transversality condition:

$$\dot{\lambda}_i = -\frac{\partial f_i}{\partial X_i} \lambda_i, \quad \lambda_i(t_f) = 0$$

The only solution to this problem for any finite value of  $\partial f_i / \partial X_i$ , is  $\lambda_i \equiv 0$ .

Second, we note that if there is only one state equation, then the necessary conditions can be used to eliminate the adjoint variable and thus the problem reduces from a functional optimization problem to a function one. To see this, consider

$$\dot{X} = f(X, U)$$

$$J = \int_0^{t_f} f_0(X, U) dt$$

We have

$$H = -f_0 + \lambda f$$

$$\dot{\lambda} = \frac{\partial f_0}{\partial X} - \lambda \frac{\partial f}{\partial X}$$

Applying the MP (assuming for the moment unbounded optimal control exists)

$$H = -f_0 + \lambda f = 0$$

$$\frac{\partial H}{\partial U} = -\frac{\partial f_0}{\partial U} + \lambda \frac{\partial f}{\partial U} = 0$$

Eliminating  $\lambda$  gives

$$-\frac{\partial f_0}{\partial U} f + \frac{\partial f}{\partial U} f_0 = 0$$

for the optimal control. Alternatively, a direct approach may be used:

$$J = \int f_0 dt = \int \frac{f_0}{f} dX$$

Thus  $(f_0/f)$  is to be minimized with respect to  $U$  at constant  $X$ ; this leads directly to the equation for optimal control derived just above from the MP.

SPT provides an organized, mathematical way to view order reduction of differential equations. Consider the initial value system

$$\dot{X} = f(X, Y) \quad X(0) = X_0$$

$$\varepsilon \dot{Y} = g(X, Y) \quad Y(0) = Y_0$$

where  $\varepsilon$  is a “small” parameter.

Since  $\varepsilon$  is small, an approximate system may be expected to be

$$\dot{X}_r = f(X_r, Y_r)$$

$$0 = g(X_r, Y_r)$$

It can be proved that under certain conditions, the solution of this problem is a good approximation to the solution of the original problem, except near  $t = 0$  because the boundary condition  $Y(0) = Y_0$  will be generally violated these.

The problem is that  $Y$  undergoes a rapid transition from its boundary condition to the approximate solution at  $t = 0$ . To analyze this motion, the time scale is stretched by  $T = t / \varepsilon$ . The resulting equations are called the boundary layer equations

$$\frac{dX}{dT} = \varepsilon f(X, Y)$$

$$\frac{dY}{dT} = g(X, Y)$$

Setting  $\varepsilon = 0$  to approximate these equations

$$\frac{dX}{dT} = 0 \Rightarrow X = \text{const} = X_0$$

$$\frac{dY_b}{dT} = g(X_0, Y_b)$$

The solution to this equation approximates the desired solution near  $t = 0$ . There are matching techniques to combine these two solutions to give an over-all approximation, if desired. The key observation is that a second order system has been replaced by two first order systems, and each of them reduces to a function optimization problem.

The SPT provides a convenient way to look at the energy state approximation. Define the aircraft energy per unit weight by

$$E = h + \frac{1}{2g} V^2$$

Differentiate and use the state equations in the Appendix

$$\dot{E} = \dot{h} + \frac{V}{g} \dot{V} = \frac{V(T_v - D)}{Mg} = P$$

Where  $T_v$  is the component of thrust along  $\underline{V}$  and  $P$  is the specific excess power. Note that this equation is valid for all three sets of equations given in the Appendix.

Now replace  $V$  by  $E$  as state variable and use the observation that  $h$  and  $\gamma$  are capable of rapid change relative to  $E$ . This motivates writing

$$\dot{E} = P$$

$$\varepsilon \dot{h} = \dots$$

$$\varepsilon \dot{\gamma} = \dots$$

Setting  $\varepsilon = 0$  then gives an order reduction of the equations of motion by two. We will use this approximation, the ESA, throughout.

This approximation has a long history of successful application in a wide variety of flight trajectory problems. The main drawback is that the variables  $h$  and  $\gamma$  may now jump instantaneously at points along the trajectory, as well as at the boundaries. These jumps could be accounted for by boundary layer analysis, but this is not done in this report.



ESA equations of motion for the three cases of interest are given in the Appendix. these equations will now be used as the basis for discussing specific trajectory optimization problems.

### **Minimum Time/Fuel to Climb**

Starting from equations (1)'

$$\dot{m} = -CT$$

$$m(0) = m_0$$

$$\dot{X} = V$$

$$\dot{E} = P$$

$$E(0) = E_0, E(t_f) = E_f$$

$$L = mg$$

$$J = \int (K_1 + K_2 CT) dt$$

Here, the system functions and boundary conditions do not depend on  $X$  and thus the equation  $\dot{X} = V$  drops out of the problem:

$$\dot{m} = -CT$$

$$m(0) = m_0$$

$$\dot{E} = P$$

$$E(0) = E_0, E(t_f) = E_f$$

$$J = \int (K_1 + K_2 CT) dt$$

with  $P$  evaluated at  $L = mg$ . The system functions and boundary conditions now depend on both  $E$  and  $M$  and hence neither state equation uncouples. Thus the MP must be applied and a 2PBVP solved.

To reduce the problem to one of function optimization, SPT is used to further reduce the system.

$$\dot{m} = -CT$$

$$\varepsilon \dot{E} = P$$

Setting  $\varepsilon = 0$  gives a single state equation

$$\dot{m} = -CT \quad m(0) = m_0$$

$$T = D, L = W$$

The optimization problem is now ( $h$  and  $E$  are controls)

$$J = (K_1 + K_2 CT) t_f$$

With the obvious trivial solution  $t_f = 0$ . Also, because the system functions do not depend on  $m$  and  $m(t_f)$  is free,  $\lambda_M \equiv 0$ .

The boundary layer system for this problem with  $\varepsilon = 0$  is simply

$$\dot{E} = P$$

with  $m = \text{const}$ , so that

$$J = \int (K_1 + K_2 CT) \frac{dE}{P}$$

and the solution reduces to

$$\max_h \left( \frac{P}{K_1 + K_2 CT} \right) \Big|_{E=\text{const}}$$

assuming that  $\frac{P}{(K_1 + K_2 CT)}$  is positive and  $E$  is monotonic. This is the well-known energy climb path.

From now on we will assume “slowly varying” mass, that is that  $m$  is on a slower time scale than  $E$  and thus its state equation may be ignored. It is also assumed that the throttle is fixed.

### **Fixed Range**

This problem is the same except that range is fixed

$$\dot{X} = V \quad X(0) = X_0, X(t_f) = X_f$$

$$\dot{E} = P \quad E(0) = E_0, E(t_f) = E_f$$

$$J = \int (K_1 + K_2 CT) dt$$

Here,  $\lambda_x = \text{const} \neq 0$  so that the  $\dot{X} = V$  state equation does not uncouple, and we have a 2PBVP. To effect system order reduction, SPT is used.

$$\dot{X} = V$$

$$\epsilon \dot{E} = P$$

$$H = -K_1 - K_2 CT + \lambda_x V + \lambda_E P$$

$$\dot{\lambda}_x = -\frac{\partial H}{\partial X} = 0 \Rightarrow \lambda_x = \text{const}$$

$$\varepsilon \dot{\lambda}_E = -\frac{\partial H}{\partial E} = K_2 \frac{\partial(CT)}{\partial E} - \lambda_x \frac{\partial V}{\partial E} - \lambda_\varepsilon \frac{\partial P}{\partial E}$$

Setting  $\varepsilon = 0$  a problem with a single state is obtained

$$\dot{X} = V$$

$$T=D$$

$$H = -K_1 - K_2 CT + \lambda_x V$$

$$L=W$$

Applying the MP:

$$\text{Min}_{h,E} \left( \frac{K_1 + K_2 CT}{V} \right)_{\substack{T=D \\ L=W}} = \frac{K_1 + K_2 C_c T_c}{V_c}$$

$$\lambda_x = \frac{K_1 + K_2 C_c T_c}{V_c}$$

This defines a cruise point, characterized by  $C_c$ ,  $T_c$ , and  $V_c$ , in the flight envelope. By proper selection of  $K_1$  and  $K_2$ , this point can be made to closely approximate minimum direct-operating-cost cruise.

For minimum time ( $K_1 = 1$ ,  $K_2 = 0$ ), the optimum cruise point is given by

$$\text{Max}_{h,E} (V)$$

For minimum fuel consumption ( $K_1 = 0$ ,  $K_2 = 1$ ) it is

$$\text{Max}_{h,E} \left( \frac{V}{CT} \right) = \text{Max}_{h,E} \left( \frac{V(l/D)}{C} \right)$$

which is the classic Brequet cruise point.

The boundary layer with  $\varepsilon = 0$  is

$$\dot{E} = P$$

$$H = -K_1 - K_2 CT + \lambda_x V + \lambda_E P$$

so that the optimal climb flight path is given by

$$\text{Max}_h \left( \frac{P}{K_1 + K_2 CT - \lambda_x V} \right) \Big|_{E=\text{const}}$$

with  $\lambda_x$  as given above.

### Maximum Turning With No Thrust

We start with (2)' with  $T=0$ .

$$\dot{X} = V \cos \chi$$

$$\dot{Y} = V \sin \chi$$

$$\dot{E} = P = -\frac{VD}{mg}$$

$$\dot{\chi} = \frac{L \sin \phi}{mV}$$

$$L \cos \phi = mg$$

with

$$J = -\int \dot{\chi} dt = -\int \frac{L \sin \phi}{mV} dt$$

In this case the  $\dot{X}$ ,  $\dot{Y}$  and  $\dot{\chi}$  equations all uncouple. Changing to more convenient variables:

$$\dot{E} = -V(B + C\omega^2)$$

$$J = -\int \omega f dt$$

where

$$\omega = \frac{\tan \phi}{\tan \phi_M}, \quad -1 \leq \omega \leq +1$$

$$\phi_M = \sec^{-1}[\min(C_L \text{ limit, load factor limit})]$$

$$f = \frac{g \tan \phi_M}{V}$$

Thus

$$J = \int \frac{\omega f}{V(B + C\omega^2)} dE$$

and the optimal controls are given by

$$\text{Max}_{h, \omega} \left( \frac{\omega f}{V(B + CW^2)} \right) \Big|_{E=\text{const}}$$

which leads to

$$\frac{\partial}{\partial \omega}(\ ) = 0 \Rightarrow \omega = \pm \sqrt{\frac{B}{C}}$$

$$\omega = \min\left(\sqrt{\frac{B}{C}}, 1\right) \quad (\text{assuming right hand turn})$$

$$\frac{\partial}{\partial h}(\ ) = 0 \Rightarrow$$

$$\left(V \frac{\partial f}{\partial h} + \frac{fg}{V}\right) (B + C\omega^2) - fV \left(\frac{\partial B}{\partial h} + \frac{\partial C}{\partial h} \omega^2\right) = 0$$

where

$$B = \frac{D_o + D_{Lo}}{Mg}, \quad C = \frac{D_{Lo} V^2 f^2}{Mg^3}$$

so that

$$\sqrt{\frac{B}{C}} = \frac{g}{Vf} \sqrt{1 + \frac{D_o}{D_{Lo}}}$$

The search for the optimum  $h$  probably should be done numerically.

Next, consider the same problem but using (3)'. Now, the  $\dot{X}$  equation uncouples but the  $\dot{y}$  and  $\dot{z}$  equations do not. The coupling is of two types. First, through the Coriolis terms, which are relatively small and can be ignored. Second, through the centripetal terms, which are large at the start of descent trajectories from orbit.

There are two ways to deal with this problem. First, the Coriolis and centripetal terms are ignored. This is justified because what is really sought is turning ability due to banking and these terms mask this. Second, the  $\dot{E}$  and  $\dot{\chi}$  terms may be decoupled using SPT.

### Maximum Cross-Range

Next consider, using (2)'

$$J = -\int \dot{Y} dt = -\int V \sin \chi dt$$

$$\dot{X} = V \cos \chi$$

$$\dot{Y} = V \sin \chi$$

$$\dot{E} = P$$

$$\dot{\chi} = \frac{L \sin \phi}{m V}$$

$$L \cos \phi = mg$$

As before, the  $\dot{X}$  and  $\dot{Y}$  equations uncouple but now the  $\dot{\chi}$  equation does not. To reduce this to a function optimization problem, further time-scale separation is required. Putting  $\dot{\chi}$  on a slower time scale than  $\dot{E}$  gives the solution  $V = 0$  and  $\lambda_x = 0$ .

Using equations (3)' results in the same problems as for maximum turning.



## Appendix

### Equations of Motion

The following are the aircraft point-mass equations of motion under various approximations.

(1) Flight in a vertical plane over a flat, non-rotating earth; no winds aloft and thrust aligned with velocity.

$$\dot{m} = -CT$$

$$\dot{X} = V \cos \gamma$$

$$\dot{h} = V \sin \gamma$$

$$\dot{\gamma} = \frac{T - D - mg \sin \gamma}{m}$$

$$\dot{\gamma} = \frac{L - mg \cos \gamma}{mV}$$

(2) 3-D flight, otherwise the same as (1).

$$\dot{m} = -CT$$

$$\dot{X} = V \cos \gamma \sin \chi$$

$$\dot{\gamma} = V \cos \gamma \cos \chi$$

$$\dot{h} = \sin \gamma$$

$$\dot{\cdot} = \frac{T - D - mg \sin \gamma}{m}$$

$$\dot{\chi} = \frac{L \sin \phi}{mV \cos \gamma}$$

$$\dot{\gamma} = \frac{L \cos \phi - mg \cos \gamma}{mV}$$

(3) 3-D flight over a spherical, rotating earth; no winds aloft, thrust not aligned with velocity, terms in the square of the earth rotation ignored.

$$\dot{m} = -\frac{T}{g_s I_{sp}}$$

$$\dot{V} = \frac{T \cos \beta \cos (\alpha + \zeta) - D}{m} - g \sin \gamma$$

$$\dot{\gamma} = \left( \frac{T \cos \beta \sin (\alpha + \zeta) + L}{mV} \right) \cos \phi - \frac{g}{V} \cos \gamma + \frac{V}{r} \cos \gamma + 2\omega \cos \chi \cos \frac{Y}{R}$$

$$\dot{\chi} = \left( \frac{T \cos \beta \sin (\alpha + \zeta) + L}{mV \cos \gamma} \right) \sin \phi - \frac{V}{r} \cos \gamma \cos \chi \tan \frac{Y}{R}$$

$$+ 2\omega \left( \tan \gamma \sin \chi \cos \frac{Y}{R} - \sin \frac{Y}{R} \right)$$

$$\dot{h} = V \sin \gamma$$

$$\dot{X} = \frac{VR \cos \gamma \cos \chi}{r \cos \frac{Y}{R}}$$

$$\dot{Y} = \frac{VR \cos \gamma \sin \chi}{r}$$

The following are the energy-state approximations of these equations.

(1)'

$$\dot{m} = -CT$$

$$\dot{X} = V$$

$$\dot{E} = \frac{V(T - D)}{mg} = P$$

$$L = mg$$

(2)'

$$\dot{m} = -CT$$

$$\dot{X} = V \cos \chi$$

$$\dot{\phantom{X}} = V \sin \chi$$

$$\dot{E} = P$$

$$\dot{\chi} = \frac{L \sin \phi}{mV}$$

$$L \cos \phi = mg$$

(3)' (with  $T = 0$  and  $m = \text{const}$ )

$$\dot{E} = -\frac{VD}{mg_s}$$

$$O = \frac{L}{mV} \cos \phi - \frac{g}{V} + \frac{V}{r} + 2\omega \cos \chi \cos \frac{Y}{R}$$

$$\dot{\chi} = \frac{L}{mV} \sin \phi - \frac{V}{r} \cos \chi \tan \frac{Y}{R} - 2\omega \sin \frac{Y}{R}$$

$$\dot{X} = \frac{VR \cos \chi}{r \cos \frac{Y}{R}}$$

$$\dot{Y} = \frac{VR \sin \chi}{r}$$

## **Appendix C**

# **Minimum Heating Re-Entry Trajectories for Advanced Hypersonic Launch Vehicles**

**February 5, 1997**

**M.S. Thesis  
Santa Clara University**

**by  
Robert Windhorst**